Measurement of the $K^+_{\mu 3}$ decay spectrum and form factors

R. Whitman* and R. J. Abrams
University of Illinois at Chicago Circle, Chicago, Illinois 60680

A. S. Carroll, T. F. Kycia, K. K. Li, D. N. Michael, P. M. Mockett,† and R. Rubinstein‡
Brookhaven National Laboratory, Upton, New York 11973

A. Wattenberg
University of Illinois at Urbana-Champaign, Urbana, Illinois 60018

(Received 8 June 1979)

The Dalitz-plot density of a sample of 3973 $K^+_{\mu 3}$ decays in flight at 1.8 GeV/c ($K^+ \to \pi^0 \mu^+ \nu_\mu$) was studied to determine λ_+ and λ_0, the linear coefficients of the t dependence of the vector and scalar form factors, where t is the four-momentum transfer to the lepton pair. The μ^+ was detected by scintillator hodoscopes, identified by thick-plate optical spark chambers and momentum analyzed in a magnetic spectrometer. The π^0 was detected by its decay into two γ's which converted in a lead–optical-spark-chamber–scintillator sandwich detector. The measured coefficients were $\lambda_+ = 0.050 \pm 0.013$ and $\lambda_0 = 0.029 \pm 0.011$. The χ^2 of the fit was 63 for 57 degrees of freedom.

I. INTRODUCTION

The semileptonic decay of the K meson has been of particular interest for several reasons. In $K \to \pi l \nu$, the K-π hadronic current is isolated from the effects of other strongly interacting particles. This is in contrast to K-nucleon scattering or production of kaons by hadron-hadron collisions. Measurements of decay rates, branching ratios, energy spectra, and lepton polarizations permit detailed comparisons with theoretical predictions based on the nature of the interaction and on specific theoretical models. Comparison of muonic and electronic decays provides a test of μ-e universality. Relationships between charged- and neutral-K-meson semileptonic decays yield information about the isotopic spin structure of the interaction. The transverse polarization of the muon allows a test of T invariance. The lepton charge asymmetry in K^0 semileptonic decay is of interest in CP violation.

The experimental determinations of the spectra, polarizations, and branching ratios have had a long history of inconsistency, both in comparisons of results using similar measurements and in comparisons between the various measurement techniques (spectra, polarizations, etc.). A considerable achievement in unification of the parametrization was made in a review and compilation by Gaillard and Chounet.[1] In a recent review Pondrom[2] analyzes kinematic and systematic effects which may have contributed to past inconsistencies.

In $K^0 \to \pi l \nu$ high-statistics (~10^6 events) results have been reported on the spectra[3] and polarization[4]; in $K^+ \to \pi l \nu$ the statistics have been limited to a few thousand events per experiment. In the present experiment we analyze the Dalitz-plot density of a sample of some 4000 $K^+ \to \pi^0 \mu^+ \nu$ decays in flight. With comparable statistics to previous experiments, this measurement is useful as an independent addition to the K^+-decay spectra experiments. We discuss the parametrization in Sec. II and the apparatus in Sec. III. In Sec. IV and Sec. V we describe the data reduction, analysis, and results. The conclusions and comparisons to other results are in Sec. VI.

II. DALITZ-PLOT DENSITY PARAMETRIZATION

The matrix element for $K^+_{\mu 3}$ decay, expressed in the current-current form, contains the product of hadronic and leptonic currents. Experimental evidence[1] supports the assumption of the Cabibbo theory that only the vector part contributes to the hadronic current. Since $\Delta Q = \Delta S = -1$, we denote the strangeness-changing vector current by V^-_α, and the matrix element is then

$$M = (G/\sqrt{2}) \sin\theta_C \bar{u}_\mu \gamma_\alpha (1+\gamma_5) u_\nu \langle \pi^0 | V^-_\alpha | K^+ \rangle . \quad (2.1)$$

It is customary to choose the sum and difference of the kaon and pion four-momenta (k and q) as basis vectors to write the hadronic current as

$$\langle \pi^0 | V^-_\alpha | K^+ \rangle \propto (k+q)_\alpha f_+(t) + (k-q)_\alpha f_-(t) ,$$

where $t = (k-q)^2$ is the four-momentum transfer to the lepton pair. The decay rate is given by $|M^2|$ from Eq. (2.1), summed over lepton spin states, so that in the kaon center-of-mass (c.m.) system the Dalitz-plot density is

$$\rho(E_\pi, E_\mu) \propto A f_+^2(t) + B f_+(t) f_-(t) + C f_-^2(t) . \quad (2.2)$$

The functions $f_+(t)$ and $f_-(t)$ are form factors and the terms A, B, and C are functions of the kinematic variables. In the c.m. system

$$A \equiv M_K(2E_\mu E_\nu - M_K E_\pi^*) + m_\mu^2\left(\frac{E_\pi^*}{4} - E_\nu\right),$$

$$B \equiv m_\mu^2\left(E_\nu - \frac{E_\pi^*}{2}\right),$$

$$C \equiv m_\mu^2\left(\frac{E_\pi^*}{4}\right),$$

where

$$E_\pi^* \equiv \frac{M_K^2 + m_\pi^2 - m_\mu^2}{2M_K} - E\ .$$

We assume that f_+ and f_- are relatively real in accord with time reversal invariance.[1]

Conventionally, $f_+(t)$ is expanded in t as

$$f_+(t) = f_+(0)\left[1 + \lambda_+\left(\frac{t}{m_\pi^2}\right) + \cdots\right]. \tag{2.3}$$

Owing to the limited range of t kinematically allowed and the statistical uncertainty of the present data, we need to retain only the first-order term in Eq. (2.3). This equation to first order then defines a new parameter λ_+ which characterizes the linear t dependence of $f_+(t)$. It has been pointed out[1,3] that another form factor may be defined,

$$f_0(t) \equiv f_+(t) + \frac{t}{M_K^2 - m_\pi^2} f_-(t) \tag{2.4}$$

with a similar power-series expansion,

$$f_0(t) = f_0(0)\left[1 + \lambda_0\left(\frac{t}{m_\pi^2}\right) + \cdots\right]. \tag{2.5}$$

Retaining only the first-order term carries the implicit assumption that the t dependence of f_- is small.

In polarization experiments the measurement is sensitive to the ratio of the form factors

$$\xi(t) \equiv \frac{f_-(t)}{f_+(t)}\ .$$

Using the first-order terms of Eqs. (2.3) and (2.5), and the definition in Eq. (2.4),

$$\xi(t) = \frac{M_K^2 - m_\pi^2}{m_\pi^2}\left[\frac{\lambda_0 - \lambda_+}{1 + \lambda_+(t/m_\pi^2)}\right].$$

At $t = 0$, a relation between three experimentally determined parameters is obtained:

$$\xi(0) = \frac{M_K^2 - m_\pi^2}{m_\pi^2}(\lambda_0 - \lambda_+). \tag{2.6}$$

We have made fits to the Dalitz-plot density and the π^0 energy spectrum in terms of the parameters (λ_+, λ_0) and in terms of $(\lambda_+, \xi(0))$. As shown in Sec. V, the (λ_+, λ_0) parameters are less strongly correlated than the $(\lambda_+, \xi(0))$ parameters, and are thus a better set of parameters for our results. The $(\lambda_+, \xi(0))$ fits are useful for comparison to polarization experiments.

III. APPARATUS

A partially separated 1.8-GeV/c K^+ beam, from the G-10 target at the Brookhaven Alternating Gradient Synchrotron (AGS), was used. Typically, the beam intensity was 8×10^4 K^+ per pulse, with a K/π ratio approximately unity. A differential Cerenkov counter[5] provided a K^+ signal which had a π contamination of about 0.1%.

The apparatus is shown in Fig. 1. A spectrometer, consisting of wire spark chambers (WSC1–14) and a 48 in. × 48 in. × 18 in. 3 kG magnet, was used to determine the incident K^+ direction, the decay μ^+ momentum and angle. The decays occurred in a He-filled decay region shown in Fig. 1. A γ detector consisting of Pb, scintillators, and optical spark chambers[6] was used to detect the two γ's from the π^0 decay. The spectrometer and γ detector were used in other experiments ($K^\pm \to \pi^\pm\pi^0\gamma$, $K^\pm \to \pi^\pm\gamma\gamma$, and $\pi^0 \to 4\gamma$) and have been described previously.[7]

To identify the muon and to suppress backgrounds from other decay modes, a Pb absorber and a stack of thick-plate aluminum optical spark chambers were installed downstream from the spectrometer. The absorber–range-chamber system consisted of two 8 × 8 ft spark chambers, each with seven 1-in.-thick aluminum plates, and two 6 ft × 6 ft spark chambers, each with ninety-three 0.25-in.-thick aluminum plates. A 14-in.-thick wall of Pb was installed between the two 8 ft × 8 ft spark chambers.

A "$K_{\mu 3}$" trigger signal consisted of a beam K signal, two or more counts in the γ detector, and a count in each of two scintillation-counter hodoscopes, denoted π and μ hodoscope in Fig. 1. The

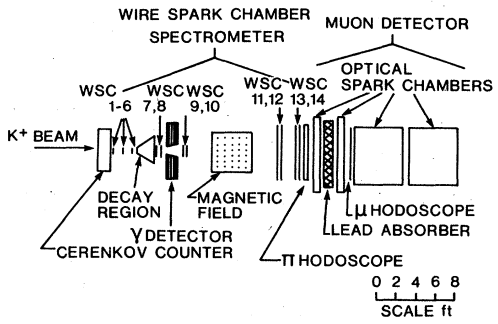

FIG. 1. Apparatus. Lead-scintillator veto counters near decay region are not shown.

γ-detector electronics provided a single count from each contiguous group of sectors, thus eliminating multiple counts due to shower spreading. Anticoincidence counters (not shown in Fig. 1) were used around the decay region to suppress triggers due to events with extra γ's.

The γ detector covered a 5 ft $\times$ 5 ft area, with a conical hole in the center for passage of charged particles. The polar laboratory acceptance angle ranged from 14° to 45°. Shower origin measurements in the optical-spark chambers provided information on the γ angles and from the lengths of the showers a crude measure of the γ energies was obtained. The measured detection efficiency,[6] including scanning efficiency, is shown in Fig. 2. Below 150 MeV the detection efficiency is dominated by scanning losses; e.g., the calculated conversion efficiency is 98.3% at 50 MeV. Above 150 MeV the detection efficiency is consistent with the conversion efficiency. A detailed study of the detection efficiency and energy resolution was performed on a sample of $K^{\pm} \to \pi^{\pm}\pi^0$ decays.[6] The spread in shower penetration depth for typical γ energies was $\pm 32\%$.

Two other trigger modes were employed for calibration purposes. A "$K_{\pi 2}$" trigger signal was produced by omitting the μ hodoscope requirement. The resulting data sample included several decay modes, but was dominated by $K_{\pi 2}$ events. A "$K_{\mu 2}$" trigger signal was produced by omitting the γ-detector requirements. This sample was dominated by $K_{\mu 2}$ events. In this sample the beam momentum was lowered to 1.5 GeV/c to give a sample of muons of approximately the same laboratory momentum as those from $K_{\mu 3}$ at 1.8 GeV/c.

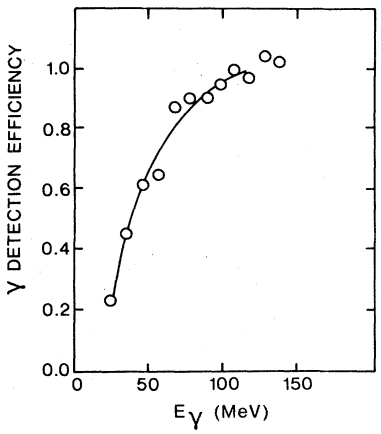

FIG. 2. Measured detection efficiency of the γ detector.

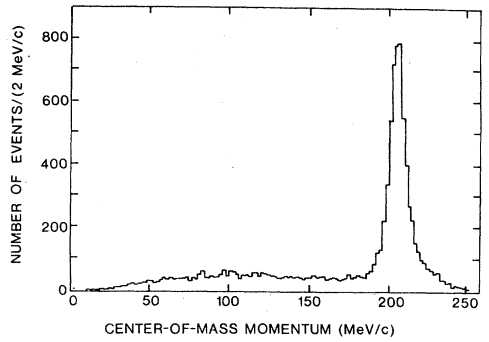

FIG. 3. c.m. momentum spectrum for "$K_{\pi 2}$" triggers.

IV. DATA REDUCTION

A. Scanning and measurement

Using the information from the wire chambers, the center-of-mass momentum of the charged particle was reconstructed. A momentum spectrum for the "$K_{\pi 2}$" triggers is shown in Fig. 3. The full width at half maximum (FWHM) of the $K_{\pi 2}$ peak (at $p_{\pi} = 205$ MeV/c) is 12 MeV/c. The three-body decays appear as the continuous spectrum. A momentum spectrum for the "$K_{\mu 3}$" triggers is shown in Fig. 4. Although there is a substantial reduction of the $K_{\pi 2}$ peak, some persist due to the presence of pion "punch throughs" and π-μ decays in flight.

For the sample of $K_{\mu 3}$ triggered events in which the WSC spectrometer data gave acceptable tracks and a decay vertex, photographs of the range-chamber system were scanned for events in which a charged track passed through the 8 ft $\times$ 8 ft spark chambers and the absorber, and stopped in

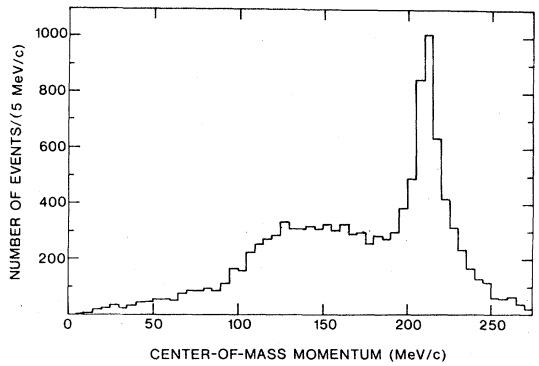

FIG. 4. c.m. momentum spectrum for "$K_{\mu 3}$" triggers for which were required a $K_{\pi 2}$ signal and a count in the μ hodoscope after the Pb absorber. The $K_{\pi 2}$ peak is shifted from 205 to ~212 MeV/c as muon mass rather than pion mass is used.

the 6 ft × 6 ft spark chambers (the range chambers). In addition, in conjunction with a determination of the muon polarization,[8] not reported here, a kink at the end of the muon track, which signified the μ-e decay of the stopped muon, was required.

After measurement, the muon track in the first optical-spark chamber was required to match the track in the wire spark chambers. To suppress further backgrounds from other K decay modes, the measured range of the muon was required to be within 20% of the range calculated from the momentum measured in the spectrometer. The FWHM of the observed range-momentum distribution was 8%.

For the events for which the spectrometer reconstruction was acceptable and for which a satisfactory muon track was measured, a scan was made of the photographs of the γ-detector optical spark chambers. Frames were measured if two or three γ-ray showers appeared in the photographs. Agreement was required between the reconstructed γ positions and the recorded sectors of the scintillation counters in the γ detector. Measurements included the coordinates of each γ conversion point and an estimate of the length of each shower based on the first and last spark-chamber gaps that showed sparks along the shower.

The total data sample consisted of approximately 800 000 "$K_{\mu 3}$" triggers, with about half for each spectrometer magnet polarity. Approximately 300 000 were reconstructed in the spectrometer. About 30 000 muon tracks were measured and about 17 000 of these matched and passed the range-momentum test. γ-detector measurements yielded about 14 000 completely measured event candidates.

B. Kinematics tests and ambiguity resolution

The kinematical quantities measured are the K^+ four-momentum, the μ^+ four-momentum, and the γ directions. The γ energies are so poorly known that they are not used directly in the kinematical reconstruction. Since the neutrino is undetected, the resulting kinematic reconstruction is a zero-constraint fit for $K_{\mu 3}$, with a twofold ambiguity in the reconstructed π^0 energy.

These measured quantities are sufficient to yield a three-constraint (3C) fit to the $K_{\pi 2}$ hypothesis; by computing a value of $\chi_{3C}{}^2$ for each $K_{\mu 3}$ candidate it is possible to remove the $K_{\pi 2}$ events in which the π^+ has "punched through" the absorber. A distribution in $\chi_{3C}{}^2$ is shown in Fig. 5; all events with $\chi_{3C}{}^2 < 20$ are rejected as $K_{\pi 2}$ decays. The result of this cut is shown in Fig. 6; the peak

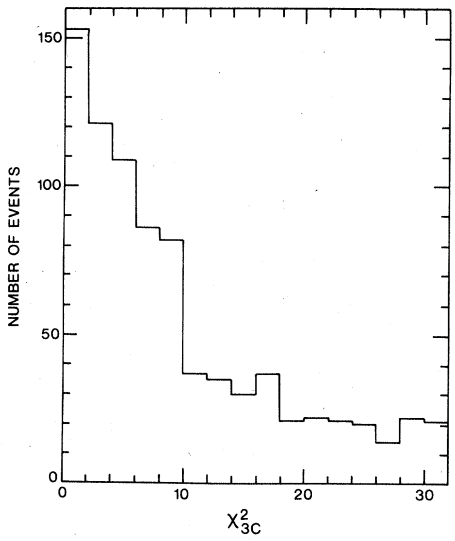

FIG. 5. Distribution in χ^2 of the 3C fit to the $K_{\pi 2}$ hypothesis. It is a 12-parameter fit.

in the muon momentum spectrum near 212 MeV/c appears to be eliminated. However, as seen in Fig. 7(a) the π^0 energy spectrum after the $\chi_{3C}{}^2$ cut shows a small peak near 110 MeV, indicating the presence of $K_{\pi 2}$ contamination. It is possible to construct a 2C fit to $K_{\pi 2}$ without using the measured value of the charged-particle momentum. Such a fit is useful to eliminate $K_{\pi 2}$ events in which the π^+ decays in flight before the charged decay particle momentum is established. After application of a 2C $K_{\pi 2}$ fit, the π^0 energy spectrum is shown in Fig. 7(b). It is apparent that the $K_{\pi 2}$ peak is essentially eliminated.

The sample of about 14 000 completely measured events is reduced to 10 131 after recon-

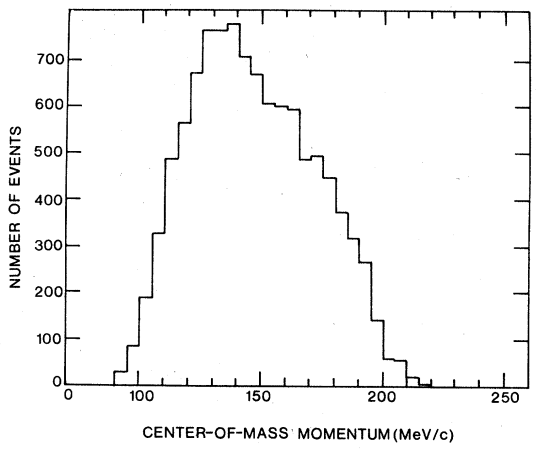

FIG. 6. Center-of-mass muon momentum spectrum for events with $\chi_{3C}{}^2 > 20$ (surviving the 3C $K_{\pi 2}$ cut).

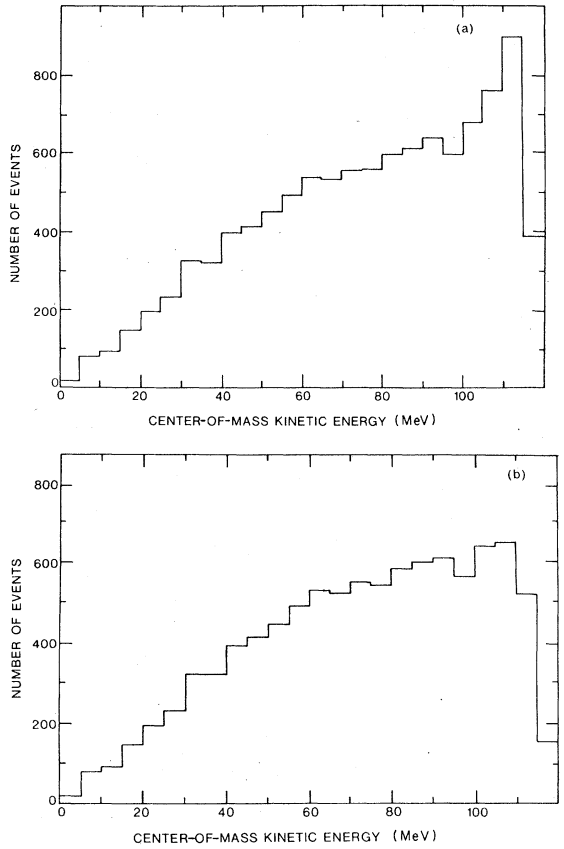

FIG. 7. Center-of-mass π^0 kinetic-energy spectrum. (a) Events with $\chi_{3C}^2 > 20$ (3C fit to $K_{\pi 2}$ rejected). (b) Events with both $\chi_{3C}^2 > 20$ and $\chi_{2C}^2 > 20$.

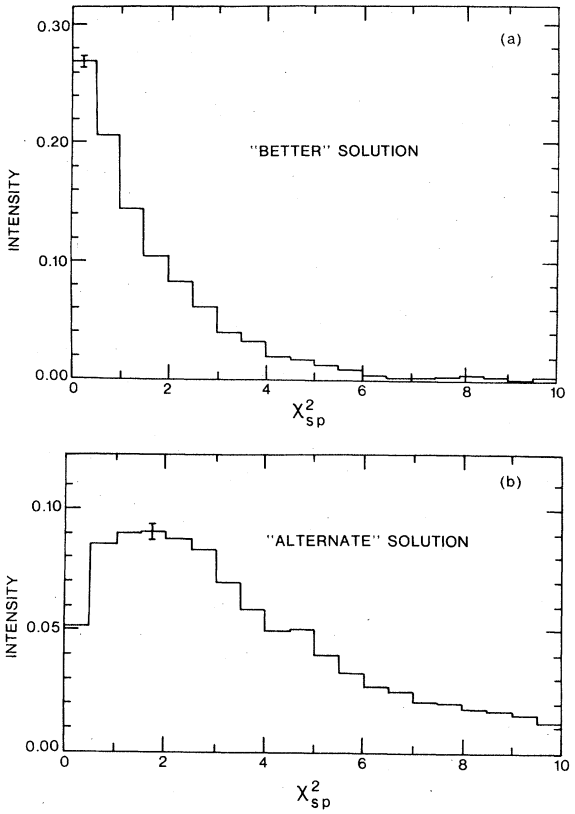

FIG. 8. Normalized distribution of χ^2 of expected versus measured shower penetration lengths for the two γ rays measured in each event. The two kinematic solutions result in two values of χ_{sp}^2 for each event. (a) The "better" value and (b) the "alternate" value, as defined in the test, are plotted separately.

struction and fiducial-volume cuts. The sample is further reduced to 8579 after application of the 2C and 3C fits to the $K_{\pi 2}$ hypothesis.

To resolve the twofold ambiguity in the $K_{\mu 3}$ kinematics the shower penetration measurements were utilized. From the kinematic solutions, the two possible laboratory energies of the π^0 were used, along with the two γ laboratory angles, to predict two pairs of γ-ray energies. From these energies and the calibration data on the γ detector,[6] corresponding values of the expected shower lengths for the pair of γ's for each solution were calculated. For each solution a χ^2 value was constructed (denoted χ_{sp}^2 for shower pair) as a comparison between the pair of expected shower lengths and the two measured shower lengths. The kinematic solution that had the lower value of χ_{sp}^2 is denoted the "better" solution; the other solution is denoted the "alternate" solution. Distributions in χ_{sp}^2 are shown in Fig. 8. Accepted events were required to have $\chi_{sp}^2 \leq 6$ for the better solution, a 5% confidence level. If the alternate solution had $\chi_{sp}^2 > 6$ the ambiguity was considered to be resolved; the alternate solution was discarded and the better solution was used. If the alternate solution also had $\chi_{sp}^2 \leq 6$, then the kinematic ambiguity was considered unresolved. However, this unresolved sample contained events for which the two solutions resulted in values of c.m. π^0 energy that differed by less than 15 MeV and hence were nearly the same; these events were included in the final data sample (the better solution was used).

After application of the χ_{sp}^2 tests to the 8579 $K_{\mu 3}$ candidates and $\Delta E_\pi < 15$ MeV cut to the unresolved sample a total of 5929 useful events remained. A Dalitz-plot distribution of the 5929 event sample is shown in Fig. 9. The double border defines the region of the Dalitz plot which was used for fitting the form factors. This region contains 3973 events.

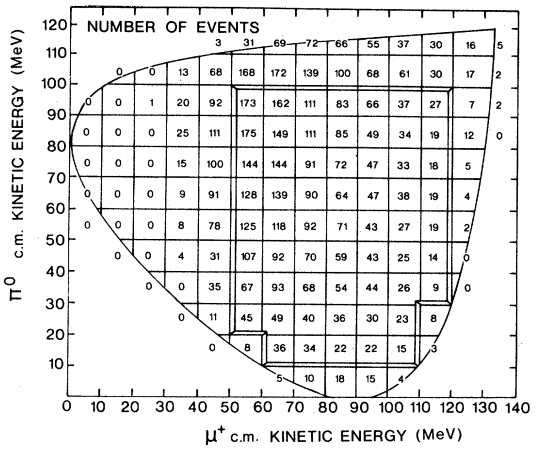

FIG. 9. Dalitz-plot distribution of final data sample. The double border encloses the 3973 events used in the final fits.

V. DALITZ-PLOT ANALYSIS

A. Acceptance calculation

A sample of $K_{\mu 3}$ decays was generated by Monte Carlo techniques. A sample of events which could be "detected" by our apparatus was obtained. For each bin of the Dalitz plot the ratio of the number of events "detected" to the number of events generated in that bin determined the acceptance. Some of the features of the acceptance calculation are described here. More details are in Ref. 8.

The K^+ momentum and direction parameters were taken from a sample of measured beam tracks. The generated c.m. energy distributions were weighted by a density distribution that corresponded to a vector current with $\xi = 0$. Measurement errors, multiple scattering, range straggling, and a simulation of the $\mu \to e$ decay were included in the μ^+ acceptance simulation. Shower spreading, shower length, detection efficiency, and measurement errors were included in the γ acceptance.

A 3C fit and a 2C fit to the $K_{\pi 2}$ hypothesis were carried out to eliminate $K_{\mu 3}$ events that would have been removed from the data sample by this procedure. The procedure outlined in Sec. IV to resolve the kinematical ambiguity was applied to the Monte Carlo generated sample, so that systematic effects of the procedure could be accounted for. After cuts and tests, a sample of 12650 events were accumulated as the accepted Monte Carlo sample (which corresponds to the 3973 data events shown in Fig. 9). Figure 10 shows plots of typical laboratory distributions for data and Monte Carlo samples. These plots are insensitive to the form factors. In Fig. 10(c) the dip near 1200 MeV corresponds to events lost due to a dead region between the two range chamber units. The dip is more pronounced in Fig. 10(b). Events in which the muon stopped within 3 in. of the center region were removed as a part of the fiducial volume cuts.

The acceptance is shown for each bin of the Dalitz plot in Fig. 11. The double line indicates the border around the region used in the data analysis. One sees a sharp decrease in acceptance below 50 MeV of μ kinetic energy, which is caused by the triggering requirement that the muon have sufficient laboratory energy to pass through the absorber. Bins that included the boundary curve of the Dalitz plot were omitted and the region with π^0 energy between 100 MeV and 110 MeV was omitted due to possible residual contamination by $K_{\pi 2}$ background. This point is discussed in more detail in Sec. VC below.

A consequence of the decrease to zero of the acceptance for μ^+ kinetic energies below 50 MeV can be seen in Fig. 11. The accepted phase-space region for large π^0 energies is reduced more than that for lower π^0 energies. This results in a sample that is relatively rich in the lower π^0 energy region which is more sensitive to the form factors. (The same effect can be seen in Fig. 7 in which the observed π^0 energy spectrum appears to flatten out at high energies.) We note that within the region we used, shown by the double border of Fig. 11, the average acceptance is constant to within approximately $\pm 10\%$ as a function of π^0 energy.

B. Results

The 3973 events in the defined region of the Dalitz plot shown in Fig. 9 were corrected for acceptance by dividing each bin of Fig. 9 by the value of the acceptance for the corresponding bin of Fig. 11, and then normalizing to obtain the same total number of events as in the original data sample. The theoretical Dalitz-plot density was fitted to the corrected data and the best-fit values of the parameters λ_+, λ_0 were obtained by χ^2 minimization. In addition the π^0 energy spectrum, integrated over muon energy, was analyzed. The π^0 energy spectrum is less sensitive than the Dalitz plot, but the acceptance calculation depends less on the simulation of the passage of the muon through the apparatus. The results of the fits for λ_0, λ_+ are shown as likelihood contours in Figs. 12(a) and 12(b). Fits for the parameters $\xi(0), \lambda_+$ are shown in Figs. 12(c) and 12(d). Our final values for the coefficients are $\lambda_+ = 0.050 \pm 0.013$, $\lambda_0 = 0.029 \pm 0.011$. These are given in Table I, together with results from the other fits.

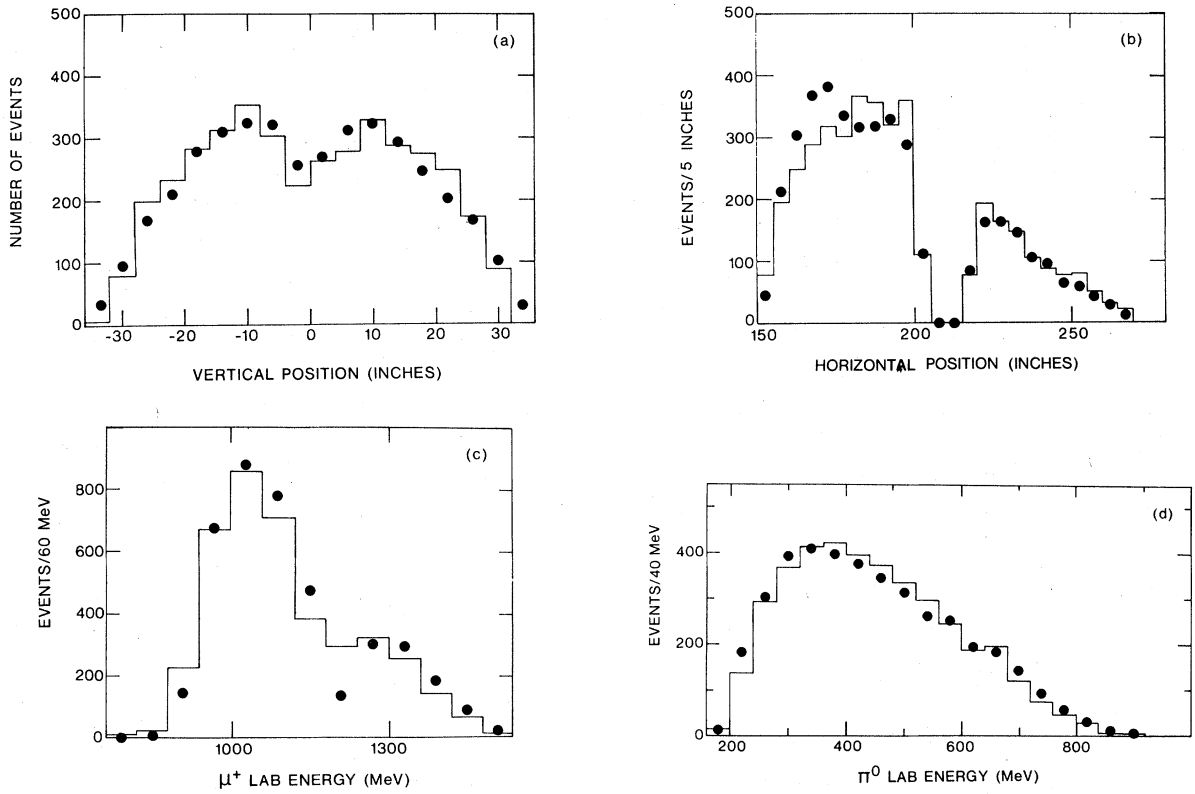

FIG. 10. Representative laboratory distributions of data sample, shown as histogram, and Monte Carlo sample, shown as dots. Data sample is derived from events within double border of Fig. 9. Monte Carlo sample is derived from events generated for acceptance calculation using $\xi(0)=0$ and $\lambda_+=0$, and afterward were weighted according to final values of form factors. These distributions are insensitive to the parameters, but show some of the characteristics of the data sample in the laboratory system. (a) Stopping point of muon in range chambers: Vertical position. The dip at the center is due to a loss of events in which tracks are obscured by spacers in the center of the range chambers. (b) Stopping point of muon in range chambers: Horizontal distance from center of analyzing magnet. The dip at 210 in. is due to a loss of events near the 2-in. thick end plates of the two range chamber units. (c) Muon laboratory energy: The dip near 1200 MeV, also due to loss near the end plate, is somewhat smeared in this variable. (d) π^0 laboratory energy.

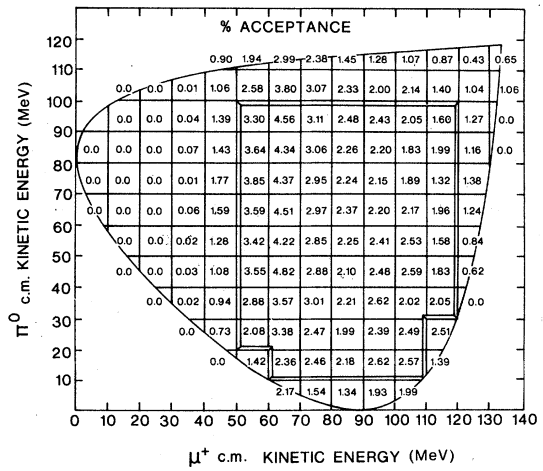

FIG. 11. Percent acceptance calculated from Monte Carlo simulation, shown per Dalitz-plot bin. Double border encloses region used in the final fits.

C. Systematics

A number of checks were made to test the stability of the results to possible systematic errors. To test the effect of selection of unambiguous events we put back in the data sample those events which had been removed in the procedure to resolve the kinematic ambiguity (see Sec. IV B and Table II). This increased the data sample to 5712 events. For the added events the lower χ_{sp}^2 solutions were used. The λ_0, λ_+ fit yielded an essentially unchanged value of λ_+, and λ_0 increased by 1 standard deviation. The confidence level remained at about 50%.

The fiducial volume for the K decay was reduced to test for possible variations in acceptance near the limits. The resulting 3482 events were refitted, with the results that λ_+ was unchanged and λ_0 was lower by 1 standard deviation. The confi-

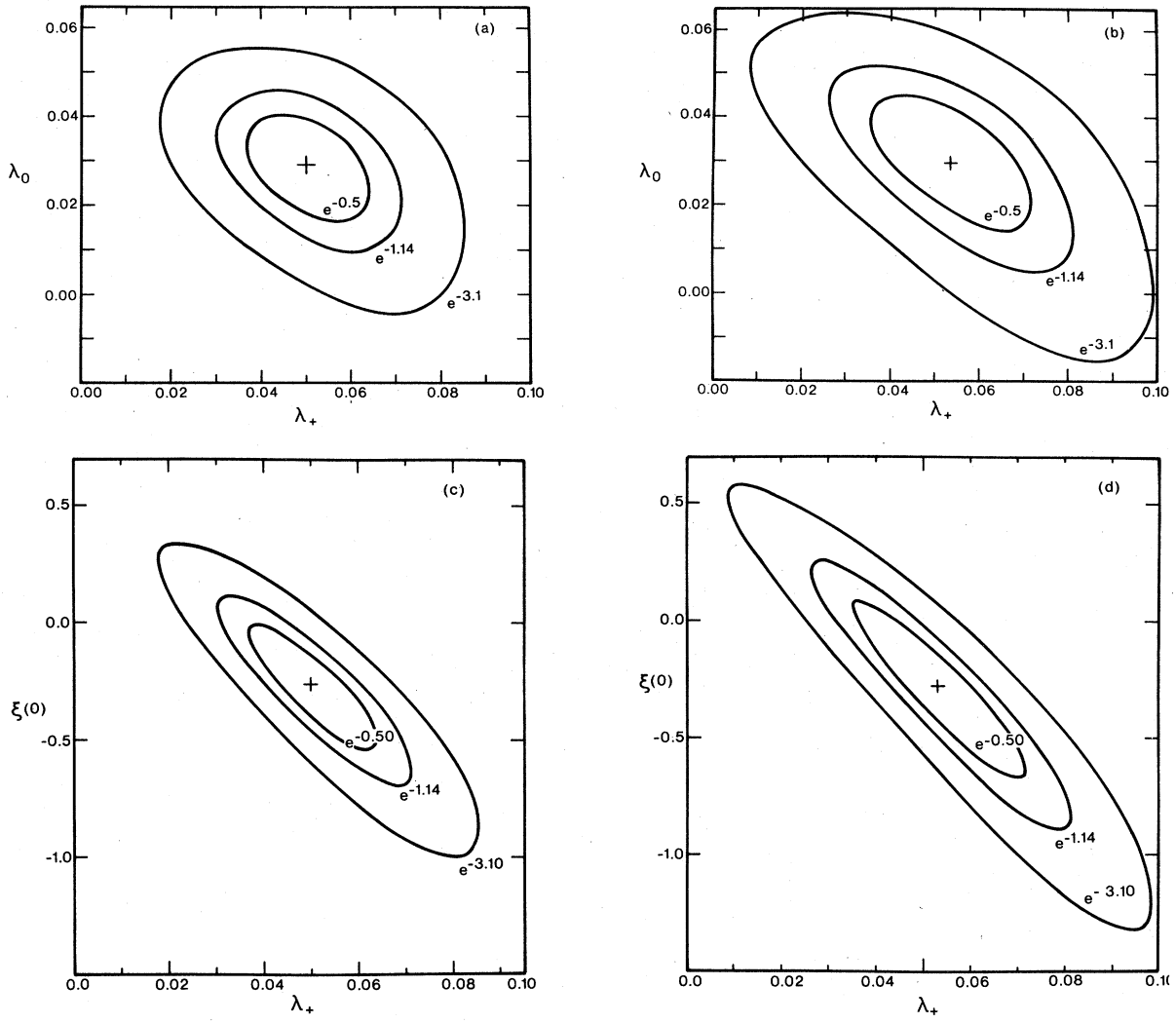

FIG. 12. Likelihood contours obtained from fits. (a) λ_0 vs λ_+ for Dalitz-plot density. (b) λ_0 vs λ_+ for π^0 spectrum. (c) $\xi(0)$ vs λ_+ for Dalitz-plot density. (d) $\xi(0)$ vs λ_+ for π^0 spectrum.

dence level dropped to 37%. (See Table II.)

The region of π^0 kinetic energy from 100 to 110 MeV was included in the data sample. The background of $K_{\pi 2}$ events with an early π-μ decay in flight was calculated by Monte Carlo methods. This background was subtracted and the π^0 energy spectrum of the resulting 4497 events was fit to determine λ_+, λ_0. The result was to increase λ_+ by 1 standard deviation; λ_0 was unchanged. (See Table II.)

TABLE I. Results of this experiment.

Method	λ_+	λ_0	$d\lambda_0/d\lambda_+$	χ^2 (DF)
Dalitz-plot density	0.050 ± 0.013	0.029 ± 0.011	-0.37	63 (57)
π^0 energy spectrum	0.053 ± 0.018	0.031 ± 0.016		5.4 (6)
Method	λ_+	$\xi(0)$	$d\xi(0)/d\lambda_+$	χ^2 (DF)
Dalitz-plot density	0.050 ± 0.010	-0.27 ± 0.25	-17	63 (57)
π^0 energy spectrum	0.053 ± 0.018	-0.27 ± 0.37		5.4 (6)

TABLE II. Summary of systematic checks.

Sample description	All results for π^0 spectrum Number of events	λ_+	λ_0	χ^2 (DF)
(a) Include events with ambiguous π^0 energy	5712	0.049 ± 0.016	0.046 ± 0.013	5.1 (6)
(b) Limited K-decay fiducial volume	3482	0.054 ± 0.018	0.015 ± 0.017	6.5 (6)
(c) Include $100 \leq E_\pi \leq 110$ MeV with background subtraction	4497	0.071 ± 0.014	0.029 ± 0.016	5.1 (7)
(d) Dalitz-plot density for sample (c)		0.062 ± 0.012	0.034 ± 0.012	80 (63)

The sensitivity of the acceptance to the shape of the generating spectrum was tested by changing its form, recalculating the acceptance, and refitting the parameters. Values of λ_+, λ_0 changed by less than 1 standard deviation.

The possibility that selection of events in which the muon decayed results in a systematic error in the spectrum was investigated by considering subsets of data according to whether the μ-e decay occurred with a forward-going or backward-going positron. The spectra in the two subsets were not significantly different.

In addition to the $K_{\pi 2}$ background discussed above, we consider several other K decay modes. The dominant decay mode, $K_{\mu 2}$, is removed by the requirement of at least two γ signals in the trigger. This was verified in that no signal at c.m. momentum of 236 MeV/c was seen in the muon spectrum to indicate a $K_{\mu 2}$ decay. K_{e3} decays were eliminated as positrons entering the Pb absorber and thick-plate optical-spark chambers were absorbed in more than fifty radiation lengths of material.

Monte Carlo studies were done on τ' ($K^+ \to \pi^0\pi^0\pi^+$) decays to determine the background from this decay mode. With the requirements that none of the four γ's hits a γ veto counter and that two γ's hit the γ detector, the expected background from τ' decays is well below 0.1%. In addition the background rate for τ' decays in which three γ's enter the γ detector was calculated and agreed with the number of three-γ events in the data. (Events with three showers were measured but were removed from the $K_{\mu 3}$ data.)

TABLE III. Compilation of results.

Reference	Experiment	Number of events	λ_+	λ_0
	$K^+_{\mu 3}$ Dalitz plot			
11	Haidt *et al.*	3240	0.050 ± 0.018	-0.011 ± 0.016 [a]
12	Chiang *et al.*	3659	-0.006 ± 0.015	0.022 ± 0.022 [b]
13	Merlan *et al.*	6527	0.027 ± 0.019	-0.025 ± 0.012
14	Braun *et al.*	1585	0.025 ± 0.017	-0.008 ± 0.020
15	Ankenbrandt *et al.*	4025	0.024 ± 0.022	-0.021 ± 0.023 [c]
	This experiment	3973	0.050 ± 0.013	0.029 ± 0.011
	K^+_{e3} Dalitz plot			
2	World average		0.0284 ± 0.0047	
	$K^0_{\mu 3}$ Dalitz plot			
3	Donaldson *et al.*	1.6×10^6	0.030 ± 0.003	0.019 ± 0.004
16	Buchanan *et al.*	3.2×10^4	0.046 ± 0.030	0.024 ± 0.013
17	Albrecht *et al.*	3.2×10^4	0.038 ± 0.007	0.045 ± 0.011 [d]
	K^0_{e3} Dalitz plot			
2	World average	6.4×10^5	0.0302 ± 0.0015	

[a] Calculated from $\xi = -0.5 \pm 0.2$, $\lambda_+ = 0.029$, $\lambda_- = 0$, and Eq. (2.6).
[b] Calculated from $\xi = -0.09 \pm 0.28$, $\lambda_+ = 0.029$, $\lambda_- = 0$, and Eq. (2.6)
[c] Calculated from $\xi = -0.62 \pm 0.28$, $\lambda_+ = 0.029$, $\lambda_- = 0$, and Eq. (2.6).
[d] Reanalyzed result; see Ref. 2.

Owing to the relatively low branching ratio for $K_{\pi\pi\gamma}$ and the low pion "punch-through" probability the background from this decay mode is estimated to be well below 0.1% of the data, also.

VI. DISCUSSION OF RESULTS

The results of this experiment are summarized in Table I. The Dalitz-plot density fits yield ($\lambda_+ = 0.050 \pm 0.013$, $\lambda_0 = 0.029 \pm 0.011$). Our results from the π^0 energy spectrum agree well with our Dalitz-plot results. There have been many theoretical calculations of the form factors in K_{l3} decay. The parameter dependence of most of the calculations makes difficult numerical comparison with our results. We refer the reader to Ref. 1 for a summary, limit our discussion to a few well known or recent theoretical values of the form factors. Our results are in agreement with the value of $\lambda_0 = +0.023$ calculated[2] from the Callan-Trieman relation.[9] In a recent parameter-free calculation by hard-meson techniques Boal and Graham[10] obtain ($\lambda_+ = 0.036$, $\lambda_0 = 0.040$) which is about 1.5 standard deviations from our values and lies on the regression path, as may be seen in Fig. 12(a). In another recent article Barut and Wilson[10] evaluate the K_{l3} form factors in closed form using rest-frame symmetry and Lorentz boosts to introduce symmetry breaking. Barut and Wilson obtain ($\lambda_+ = 0.036$, $\lambda_0 = 0.031$) which is in good agreement with our values. We also note that our value of λ_+ is about 2 standard deviations higher than the "naive" $K^*(890)$ dominance value of $\lambda_+ = m_\pi{}^2/M_{K^*}{}^2 = 0.023$.

In Table III are shown some results of Dalitz-plot experiments for $K_{\mu 3}$ and a world average[2] for K_{e3} high statistics experiments. In K_{e3} only the λ_+ parameter can be determined due to the small mass of the lepton. Our value for λ_+ is within approximately 1.5 standard deviations of the world average values of λ_+ from K^+_{e3} and K^0_{e3} experiments. We note that the values of λ_+ and λ_0 from the $K^+_{\mu 3}$ Dalitz-plot experiments show a significant spread. Since the parameters λ_+ and λ_0 are correlated it is more meaningful to compare λ_0 results after extrapolating to a common value of λ_+, as done by Pondrom.[2]

In Table IV are world averages[2] for λ_0 including polarization experiments on $K_{\mu 3}$ and our result, all extrapolated to $\lambda_+ = 0.03$ for comparison. For the polarization results Pondrom[2] has used the $\xi(t=0)$ value from each experiment, a $\lambda_+ = 0.030$ consistent with K_{e3} results, and Eq. (2.6) to obtain λ_0. As seen in Table IV the values of λ_0 obtained from the polarization experiments are more negative than those from the Dalitz-plot experiments. The values of λ_0 from the $K^0_{\mu 3}$ Dalitz plot are definitely positive. Our value of λ_0 agrees with the $K^0_{\mu 3}$ Dalitz-plot values and is approximately 2 standard deviations above the world average of λ_0 from the other $K^+_{\mu 3}$ Dalitz-plot determinations. By including our value of λ_0 with the other values from the $K^+_{\mu 3}$ Dalitz plot in Table IV the new world average for λ_0 (extrapolated to $\lambda_+ = 0.03$) becomes $+0.006 \pm 0.0095$, approximately 1.5 standard deviations from the world average value from $K^0_{\mu 3}$ Dalitz-plot measurements.

TABLE IV. Summary of normalized[a] results for λ_0. World averages from Ref. 2.

Experiment	λ_0
$K^+_{\mu 3}$ Dalitz plot	
World average	-0.004 ± 0.011
This experiment	0.036 ± 0.019
$K^0_{\mu 3}$ Dalitz plot	
World average	0.022 ± 0.0036
$K^+_{\mu 3}$ polarization	
World average	-0.023 ± 0.011
$K^0_{\mu 3}$ polarization	
World average	-0.012 ± 0.008

[a] All results are normalized to $\lambda_+ = 0.030$.

The agreement of our determination of λ_+ and λ_0 with that of $K^0_{\mu 3}$ Dalitz-plot experiments is in support of the $\Delta I = \frac{1}{2}$ selection rule. The consistency found between our λ_+ determination and that of K_{e3} experiment supports the μ-e universality hypothesis.

ACKNOWLEDGMENTS

We are indebted to the AGS staff for cooperation and help during the experiment. We wish to acknowledge the generous support of the UICC Computer Center during the data analysis. We thank the scanning crews at Urbana, UICC, and BNL for their efforts. We are grateful to L. Lederman for the use of the range spark chambers. The technical support of O. Thomas, G. Munoz, F. Seier, J. Fuhrmann, M. Pelafas, G. Isherwood, and J. Simone is greatly appreciated. This work was supported in part by the U. S. Department of Energy.

*Present address: Rutgers University, New Brunswick, N. J. 08903.
†Present address: University of Washington, Seattle, Wash. 98105.
‡Present address: Fermilab, Batavia, Ill. 60510.

[1]L. M. Chounet, J.-M. Gaillard, and M. K. Gaillard, Phys. Rep. 4C, 199 (1972).
[2]L. Pondrom, in *Particles and Fields '76*, proceedings of the annual meeting of the Division of Particles and Fields of the APS, edited by H. Gordon and R. F. Peierls (BNL, Upton, New York, 1977).
[3]G. Donaldson *et al.*, Phys. Rev. D 9, 2960 (1974).
[4]A. R. Clark *et al.*, Phys. Rev. D 15, 553 (1977).
[5]B. Leontic and J. Teiger, Brookhaven National Laboratory Internal Report No. BNL-50031 (T-447) (unpublished).
[6]R. J. Abrams *et al.*, Nucl. Instrum. Methods 107, 569 (1972).
[7]R. J. Abrams *et al.*, Phys. Rev. Lett. 29, 1118 (1972); 30, 500 (1973); Phys. Lett. 45B, 66 (1973); Phys. Rev. D 15, 22 (1977).
[8]Russell Whitman, Ph. D. thesis, University of Illinois at Chicago Circle, 1977 (unpublished).
[9]C. Callan and S. Trieman, Phys. Rev. Lett. 16, 153 (1966).
[10]D. H. Boal and R. H. Graham, Phys. Rev. D 15, 1878 (1977); A. O. Barut and R. Wilson, *ibid.* 19, 260 (1979).
[11]D. Haidt *et al.*, Phys. Rev. D 3, 10 (1971).
[12]I-H. Chiang *et al.*, Phys. Rev. D 6, 1254 (1972).
[13]S. Merlan *et al.*, Phys. Rev. D 9, 107 (1974).
[14]H. Braun *et al.*, Nucl. Phys. B89, 110 (1975).
[15]C. Ankenbrandt *et al.*, Phys. Rev. Lett. 28, 1472 (1972).
[16]C. D. Buchanan *et al.*, Phys. Rev. D 11, 457 (1975).
[17]K.-F. Albrecht *et al.*, Phys. Lett. 48B, 393 (1974).